ISBN: 978-3-95450-201-1 doi:10.18429/JACoW-IBIC2018-MOOB01

BEAM COMMISSIONING OF SuperKEKB RINGS AT PHASE-2

M. Tobiyama*, M. Arinaga, J. W. Flanagan, H. Fukuma, H. Ikeda, S. Iwabuchi, H. Ishii, G. Mistuka, K. Mori, E. Mulyani and M. Tejima, KEK Accelerator. Laboratory, 1-1 Oho, Tsukuba 305-0801, Japan and also SOKENDAI, Japan
G.S. Varner, U. Hawaii, Dept. Physics and Astronomy, 2505 Correa Rd., Honolulu HI 96822, USA
G. Bonvicini, Wayne State U., 135 Physics Bldg., Detroit MI 4820, USA.

Abstract

The Phase 2 commissioning of SuperKEKB rings with Belle II detector began in Feb. 2018. Staring the commissioning of positron damping ring (DR), the injection and storage of the main rings (HER and LER) smoothly continued in Apr. 2018. The first collision has been achieved on 26th Apr. with the detuned optics (200 mm x 8 mm). Performance of beam instrumentation systems and the difficulties encountered during commissioning time will be shown.

INTRODUCTION

The KEKB collider has been upgraded to the SuperKEKB collider with a final target of 40 times higher luminosity than that of KEKB. It consists of a 7 GeV high energy ring (HER, electrons) and a 4 GeV low energy ring (LER, positrons). About 2500 bunches per ring will be stored at total beam currents of 2.6 A (HER) and 3.6 A (LER) in the final design goal. After the first stage of commissioning (Phase 1) without the Belle-II detector, which started in Feb. 2016 and continued until the end of June [1, 2], we have installed the superconducting final quadrupoles (QCS) and the Belle-II detector, without innermost detectors vertex detectors such as Pixel detectors nor Silicon Vertex Detectors (VXD).

The primary target of the Phase-2 operation in accelerator side was to verify the large crossing angle, nano-beam collision scheme by squeezing the βy* smaller than the bunch length and to achieve high luminosity consistent to βy*. There also required to achieve the following conditions to proceed to the phase-3 operation by the Belle II group:

- Achieve a machine luminosity of O(10^{34}/cm^2/s) and see a clear path to further improvement.
- Examine the VXD background to verify that we can install the VXD at the start of phase 3 and then operate it for the initial first few years of phase 3.

The Phase-2 operation has started in Feb. 2018 with the commissioning of the positron damping ring (DR). The commissioning of HER and LER has started in late Mar. with detuned (non-collision) optics. After establishing the beam storage, we have jumped to the collision optics on 11th. Apr. The first collision has been observed on 26th. Apr with the IP parameter of (βx*, βy* = 200 mm, 8 mm) [3, 4].

The beam instrumentation has played a very important role at each step of commissioning, such as establishing the circulating orbit, finding the beam-beam kick, accumulating large beam currents, and so on.

In this paper we describe the results of the beam commissioning of phase 2 operation of SuperKEKB rings with the obtained performance of the beam instrumentations. The main parameters of the phase 2 operation of SuperKEKB HER/LER/DR and the types and number of main beam instrumentations are shown in Table 1.

Table 1: Main Parameters of SuperKEKB HER/LER/DR in Phase 2 Operation

	HER	LER	DR
Energy (GeV)	7	4	1.1
Circumference(m)	3016		135
Max. current (mA)	800	860	12
Bunch length (mm)	5	6	6.6
RF frequency (MHz)	508.887		
Harmonic number (h)	5120		230
Betatron tune(H/V)	44.54/ 46.56	45.54/ 43.56	8.24/ 7.17
Synchrotron tune	0.02	0.018	0.025
T. rad. damp time (ms)	58	43	12
x-y coupling (%)	0.27	0.28	10
Emittance (nm)	3.2	4.6	29
Peak luminosity	5.5x10^{33}/cm^2/s		
Beam position monitor	486	444	83
Turn by turn monitor	69	70	83
Trans. FB system	2	2	1
Visible SR monitor	1	1	1
X-ray size monitor	1	1	0
Beta. tune monitor	1	1	1
DCCT	1	1	1
Bunch current mon.	1	1	1
Beam loss monitor	105(IC)/101(PIN)		34

* email address makoto.tobiyama@kek.jp

ISBN: 978-3-95450-201-1 doi:10.18429/JACoW-IBIC2018-MOOB01

DAMPING RING COMMISSIONING

The commissioning of the posittron damping ring has started on Feb. 8th, 2018 [5]. After the tuinig of Linac to Ring beam transfer line (LTR), we have at first started to adjust the beam timinig of the BPM detectors (18K11) [6]. We have used the turn-by-turn bpm detectors based on wideband Log-ratio method. As shown in Fig. 1 the main frequency divider creates the bunch revolution timing synchronized to the injection bunch timing. For each BPM

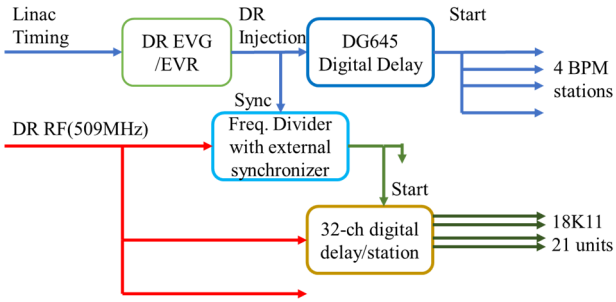

Figure 1: Block diagram of DR bpm timing system.

detectors, we have also prepaired the 32-ch digital delay unit for each BPM station [7]. As we know the relative timig differences of BPMs from the measurements of cable lengths and from the BPM locations, we simply adjusted the station timing offset measured by the injected bunch at the most upstream electrode and added individual delays. With this method, all the BPM timing have been sucessfully adjusted within 2 hours after the first injection to the ring including the tuning of the beam orbit.

Though the 18K11 has more than 32k turns of memory for each channel, it took more than 4 seconds to calculate the beam position of the 32k turns of data due to extremely poor CPU power of MVME5500. We therefore limited the processing length of the BPM waveform upto 2k turns with the software, and also made other process such as evaluating the BPM consistency on a linux cpu. With this condition, we could repeat the position measurements less than 1 second cycle.

The BPM block positions relative to the quadrupole mangents have been surveyed using FARO 3D-ARM and the results been reflected to the beam position. The mean and standard deviation of the survey was 0.07 mm ± 0.47 mm and -0.25 mm ± 0.29 mm for horizontal and vertical, respectively. The gain difference of each electrode has also been estimated by the beam-based gain mapping method [8]. It spreads rougly within 8%. The mean resolution of the BPM system with 2k sample for 1 nC/bunch beam have been estimated by the 3-BPM method to be about 2-3 μm.

By detecting the 508 MHz components from a button electrode using a 4-tap FIR cable band pass filter, we have formed a CT like monitor. The monitor worked well to find the RF timing to capture the beam. Moreover, it showed mis-timing injecting beam which is far off phased from the majority of the beam.

The output of DCCT has been measured by the Keysight 34465A with roughly 5 ksps rate coninuously without break due to data transfer. Figure 2 shows an example of measured beam current in DR with accumration time of 1 ms. Clearly it reflects imperfect step response of the DCCT circuit. The correction of the response using feed-forward method will be considered.

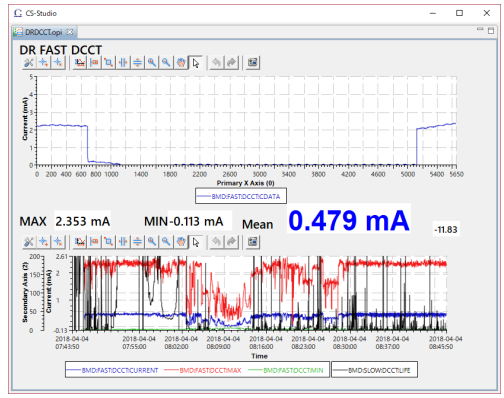

Figure 2: Example of DCCT data of DR with accumulation time of around 1 ms.

Though it is not needed to worry about the coupled-bunch instability (CBI) for DR, we have perepared a transverse bunch-by-bunch feedback system similar to the bunch feedback system to the main ring mainly to damp the residual kick of the injection and extraction kicker [9]. Using this FB system, we have also made a betatron tune mesurement system. It showed enough response even with single bunch operation. The bunch current information is also measured using the FB detector and the memory board same as the MR with reduced ring memory size.

The longitudinal and transverse beam size from the injection to the extraction have been mesured by a streak camera and a fast gated camera. Figure 3 shows an example of measured bunch length after the injection.

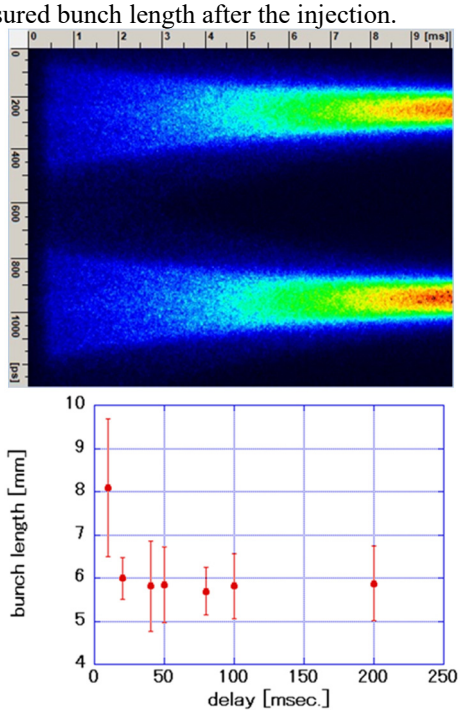

Figure 3: Measured bunch length of DR after injection.

ISBN: 978-3-95450-201-1 doi:10.18429/JACoW-IBIC2018-MOOB01

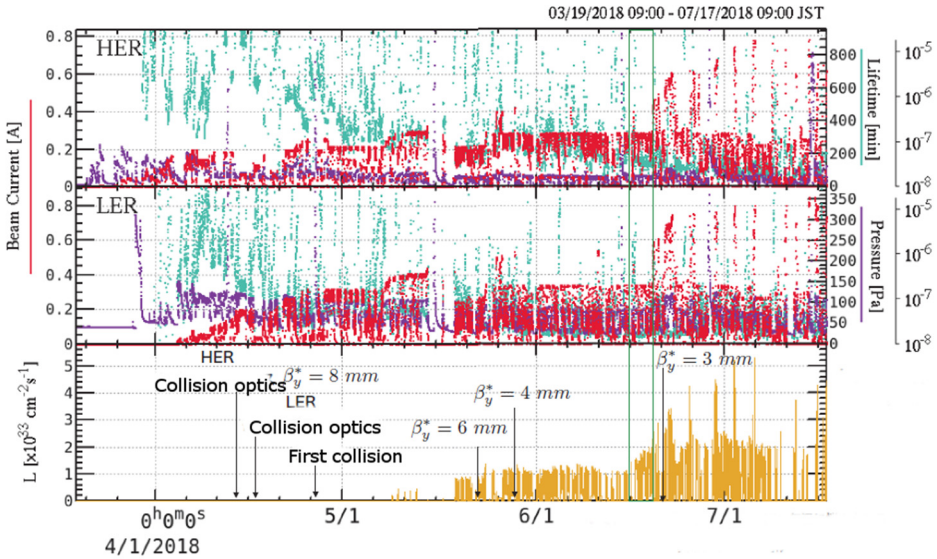

Figure 4: Beam currents and luminosity history of phase 2 operation of the SueprKEKB rings.

We have placed 34 ion chambers around the ring and the beam transport lines to measure the beam loss and also to stop the injection if the loss exceeds a threshold. The fast sample ADCs with digital peak hold circuit [10] have been used to monitor the integrated loss within 1 second.

Totally, the instruments prepeared for the DR have worked pretty well during the phase 2 operation.

HER/LER COMMISSIONING

Figure 4 shows the total history of the beam currents and luminosity of the phase 2 operation of the SuperKEKB rings. We have started the injection to HER and LER with detuned optics without local chromaticity correction section around the interaction point on late Mar. and early Apr., respectively. After establising the beam storage, we have changed the optics to the detuned collision optics and enabled the local chromaticity corrections. This jump on beam optics needed enomous efforts such as measuring the beam optics and correcting it before establishing the stable orbit. Also, we have encountered many quenches on the superconductiong coils in the final quads (QCSs). After the first collsion on 26/Apr, we graduarly tried to squieeze the betatron function to get the higher luminosity.

Gated Turn-by-Turn Monitor

Though the beam timing (definition of the bucket 0) has been shifted wildly from the phase 1 mainly due to the insertion of the damping ring in the injection timing path, the gated turn-by-turn monitors (GTBT) with fully open-gated mode worked well to detect the injection beam orbit. Newly added 19 GTBTs in the ring, especially around the HER injection points and around the collision points have helped to pass through the beam smoothly.

After establishing the beam collsion, we have re-adjusted the ADC and gate timing of the GTBTs using single bunch beam. Timing differences from phase 1 were about 920 ns and 880 ns for HER and LER, respectively.

We have newly included the offset and gain imbalance factors in the GTBTs position records. During the phase 2 operation, we have copied them from that of for the narrowband BPMs measured by employing beam based alignment (BBA) and beam based gain mappint (BBG).

The GTBTs have also routinelyl been used to reduce the residual kick of the injection kickers which helped to protect the QCS from the quench due to wild injection beam and to find the difficulties in the injection kickers such as mis-fire or timing error.

In SuperKEKB, normally the optical functions such as betatron functions, x-y couplings or dispersions have been measured by the single kick method using narrowband BPMs [11]. The GTBTs have also been used to measure the phase advances between the GTBTs, especially around the interaction point where either gain nor offsets relative to the superconducting quadrupoles are not so reliable due to fairly complexed structure and larger gain loss of the coaxial cables. Even though, for optics group the GTBTs are not so easy devices due to large size of the data. We plan to include data processing such as making FFTs, correction of one-turn delay, etc. in the IOCs for GTBTs.

The GTBTs have also used to check the orbit bump for IP dithering feedback [12]. It finds the horizontal beam offset or angle with lumosity peak at IP by slightly exciting the beam orbit with 60 to 80 Hz using air-cored magnets around IR. Figure 5 shows the measured normalized amplitude in the bump and out of the bump.

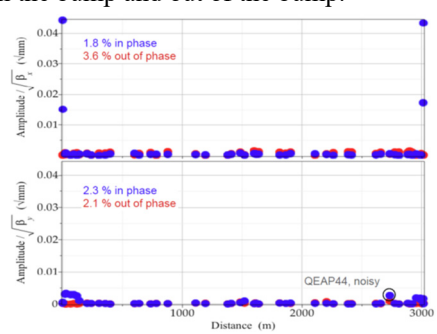

Figure 5: Normalized amplitude of dithering excitation with GTBTs. Blue dots show the in-phase componets.

ISBN: 978-3-95450-201-1 doi:10.18429/JACoW-IBIC2018-MOOB01

Clearly the dither system hardwire including the timing and tuning knob have shown the good response as expected.

IP Feedback Systems

In the nano-beam schme, though the horizontal beam-beam kick is much lower than that of normal collider, the vertical beam-beam kick is estimated to be strong enough to find the center of the collsion. We have perpared four BPM electrode set just outside the Belle II vertex chamber (QC1s). As the diameter of the vacuum chamber is only 20 mm there, we have developed special electrodes with the button diameter of 1.8 mm as shown in Fig. 6. Even with

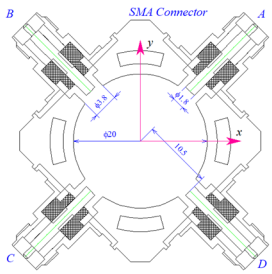

Figure 6: Special BPM electrodes for QC1.

this tiny electrode, the total power from the beam at maximum beam current is estimated to be the order of 10 W, which is similar level as that at the feedthrough of BPMs near IP in KEKB.

The vertical orbit shift at the BPMs is estimated to be several microns. A special wideband detector for the IP orbit feedback has been developed to measure the orbit at QC1s. Target performance of the detector is resolution less than 1 μm with beam current larger than 1 A and the repetition rate from 5 kHz to 32 kHz. Schematic diagram of the detector is shown in Fig. 7.

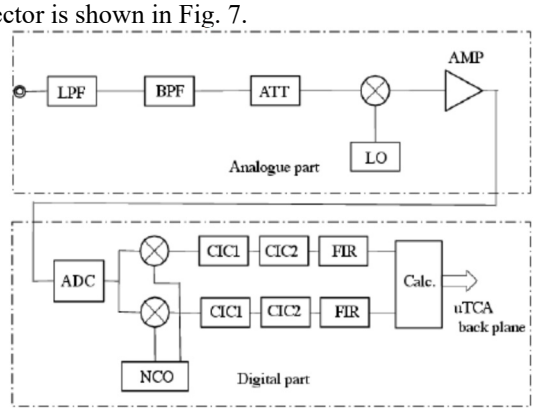

Figure 7: Block diagram of IP beam position detector.

The detector converts the 508 MHz component in BPM signal to an IF of 16.9 MHz with an analogue mixer. The IF signal is digitized by the 16-bit ADC on the mezzanine card of the microTCA card with Virtex5 FPGA (BPM unit) with the sampling frequency of 99.4 MHz, then process by a chain of digital filters (two CICs and a FIR). The cut-off frequency of the filter is 2 kHz.

The calculation of the kicks by the correctors is done by a FPGA (Virtex5) on the same microTCA shelf (DSP unit). The feedback algorithm (PID) has been designed and implemented using MATLAB/Simulink with system generator from Xilinx. Calculated kick angles for each fast steering magnets have been transferred from the DSP unit on the microTCA to the steering controller unit made of MTCA.4 through an optical fiber. The power supply controller also accepts the kick values through the network for slow correction. The BPM unit also works to output the mean beam position at QC1 as the EPICS record for COD correction and slow beam-beam kick feedback. Figure 8 shows an example of measured horizontal beam-beam kick using QC1 BPMs.

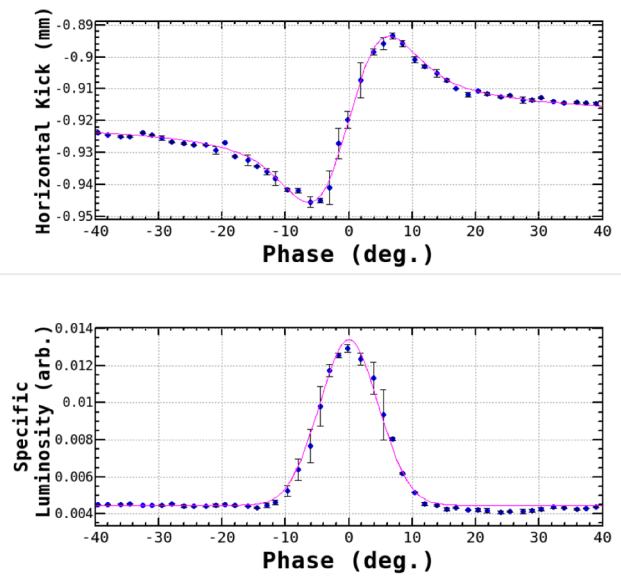

Figure 8: Example of horizontal beam-beam kick (upper) and the specific luminosity.

The resoluton has been estimated by the beam to be around 5 μm in left side (QC1LE, QC1LP), 2.5 μm in right side (QC1RE, QC1RP) with beam curren of 100 mA. The difference between left and right side comes from the signal loss due to longer cable path.

During phase 2 operation we have measured the beam based gain mapping several times. It was very strange that the gain imbalance in the QC1 BPMs were extremely lager than other BPMs, especially in QC1LP where the minimum gain coefficient was estimated to be 0.4. By the inspection and signal check during the phase 2 operation we could not find the cause of such large gain unbalance. After the phase 2 operation we will open the IP and replace the QC1 chamber assemblies and the bpm cables and try to find the cause of the gain imbalance.

Using the non-collidng and colliding beam, we have measured the slow beam vibration. Figure 9 shows an example of measured beam vibration up to 200 Hz with the beam current of around 140 mA. In the vertical plane there seem several amplitude peaks. The highest corresponds around 15 Hz with the IP comverted amplitude of around 0.16 μm which is smaller than 1/10 of vertical size at IP.

ISBN: 978-3-95450-201-1 doi:10.18429/JACoW-IBIC2018-MOOB01

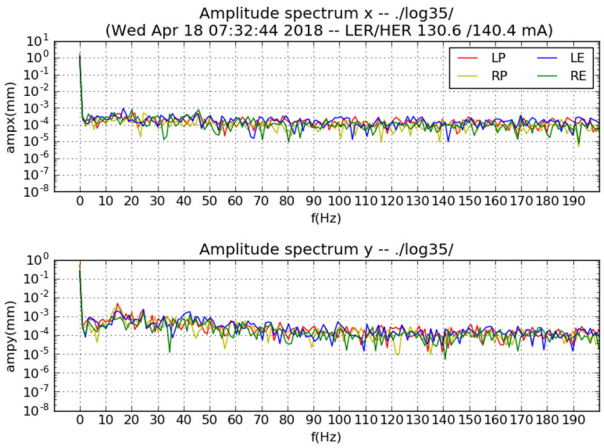

Figure 9: Measured beam vibration using QC1 BPMs with the beam current of LER/HER of 130 mA/140 mA.

We have also tried to close the vertical IP feedback and checked the beam behavior such as the beam oscillation components or luminosity by changing the gain (P) in the PID controller. Unfortunately due to overflow in a summing circuit in the controller caused by large offsets of beam position inputs it caused unexpectedly large cannonical kick. There showed no obvious change either in the beam vibration spectrum nor luminosity. Nevertheless, the system did not go unstable even with larger gain. We will change the control circuit to escape the overflow. Also with the larger vertical beam size at IP it might not be easy to check the effect of fast IP feedback. We are considering to artificially excite the vertical beam position at IP to check the effect of IP feedback.

Bunch Feedback Systems

Figure 10 shows the block diagram of the bunch-by-bunch feedback systems installed in SuperKEKB rings [9]. The system consists of position detection systems, high-speed digital signal processing systems with a base clock of 509 MHz (iGp12 [13]), and wide-band kickers fed by wide-band, high-power amplifiers.

Like the phase 1 operation, in the early stage of the commissioning of both rings we encountered very strong transverse coupled-bunch instabilities which limited the maximum beam currents. After the tuning of the timing and phase of the transverse feedback systems, we successfully suppressed the coupled-bunch instabilities up to the maximum beam current of around 800 mA with the minimum bunch separation of 4 ns.

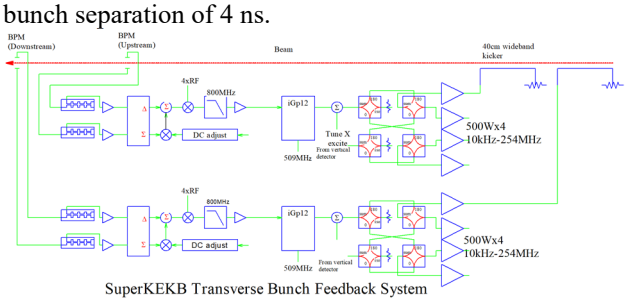

Figure 10: Block diagram of the transverse bunch feedback systems.

During the beam study of electron cloud effect (ECE) in LER we have obtained many transient domain data. Figure 11 shows an example of growing and damping transients with the 4 ns bunch separation with the beam current of 300 mA in the vertical plane. The distribution of the unstable modes and the growth time have changed drastically from the phase 1 time presumably due to the counter measure to suppress the cloud effect in the drift space.

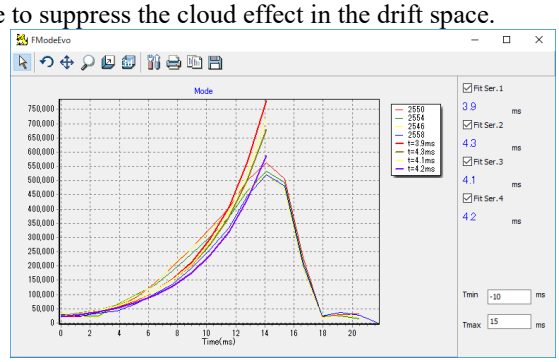

Figure 11: Evolution of vertical unstable modes with by-2 pattern in LER at a current of 300 mA. The growth time constant of mode 2550 was about 3.9 ms, which is much slower than that of obtained at phase 1. The damping time constant is estimated to be less than 1 ms, which is consistent with the phase 1 operation.

During the ECE study and the trial of high beam current at the very end of phase 2, we have encountered the longitudinal coupled-bunch instability in the LER. Though the threshold current for the nominal collision (3.06 spacing) has increased from 660 mA during the phase 1 to 800 mA, it still appeared with higher beam current. Also, the mode and threshold seemed to be affected by the setting of the head position of the vertical collimator nearest to the IP. Though we have the longitudinal bunch-by-bunch feedback systems in LER, we did not have time to tune the system. For phase 3, we will add two more longitudinal feedback cavities with 1 kW of wideband feedback amplifiers per each cavity. The longitudinal system should be tuned in the very early stage of the phase 3.

The bunch feedback related system such as the bunch current monitors, betatron tune monitors, bunch oscillation recorders have worked fine without difficulties. During the collision, we have measured the single bunch beam transfer function of a non-colliding bunch (pilot bunch) using the single bunch excitation function of the iGp12. Also, for the measurement of betatron phase advance between the GTBTs, we have excited the betatron frequency using the PLL excitation function of iGp12. Though it was not so difficult to simply excite the betatron oscillation of a pilot bunch, the beam lifetime of the bunch strongly reduced with a larger oscillation amplitude due to very narrow physical aperture in the ring. For phase 3, we are planning to implement burst beam excitation newly implemented to iGp12.

We have encountered several failures in the transverse wideband amplifiers with maximum power of 500 W due to breakdown of driver stage amplifiers. The failed amplifiers will be repaired soon. Though we have encountered

ISBN: 978-3-95450-201-1 doi:10.18429/JACoW-IBIC2018-MOOB01

several failures of high power attenuators (1.5 kW) during phase 1 operation, all the attenuators have been confirmed to be healthy after phase 2 operation.

Photon Monitors

X-ray monitors (XRMs) are installed in both rings, primary for vertical beam size measurements [14, 15]. Since the deep-Si pixel detectors and the fast readout systems developed under the US-Japan collaboration were not in time, we have used the scintillator with a CCD camera, similar to phase 1. Though during phase 1 operation, the LER XRM have shown excellent agreement with the estimation from the optical measurement (X-Y coupling), the beam size form HER XRM was not consistent with the estimation from x-y coupling nor the beam lifetime measurement due to Touschek effect.

For phase 2 operation, we have exchanged the Be filter in the HER x-ray line from 16 mm to 0.2 mm to reduce the small angle scattering in the Be. Also, we have change the vertical betatron function at the light source point from 7.6 m to 28 m. By the measurement of point spread function of X-ray beam in HER in phase 2, the scattering has confirmed to be small enough. The estimated vertical beam size was consistent with that estimated from the x-y coupling measurements.

Figure 12 shows an example of measured vertical beam size at LER during the ECE study for various filling pattern.

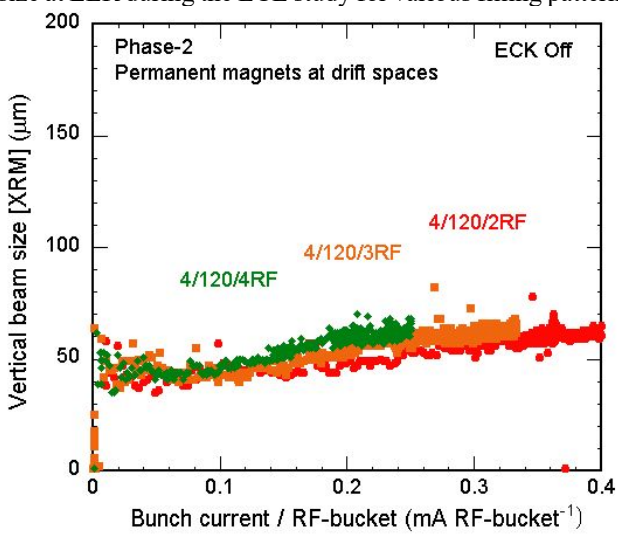

Figure 12: LER vertical beam size at ECE study.

We have also exchanged the diamond mirror in both rings for the visible SR line with 200% of larger aperture. To reduce the stray light in the visible SR line we have added baffles in the line and confirmed the effect using the laser light. With increased visible light we have tried to activate the interferometer for horizontal beam size measurements. Though in HER the system worked well, the SR spot seemed to be changed with the beam current in LER. We will open the mirror chamber to find the weak connection point around the mirror.

The bunch length has been measured using the streak camera for both rings. Figure 13 shows the measured bunch length for HER and LER.

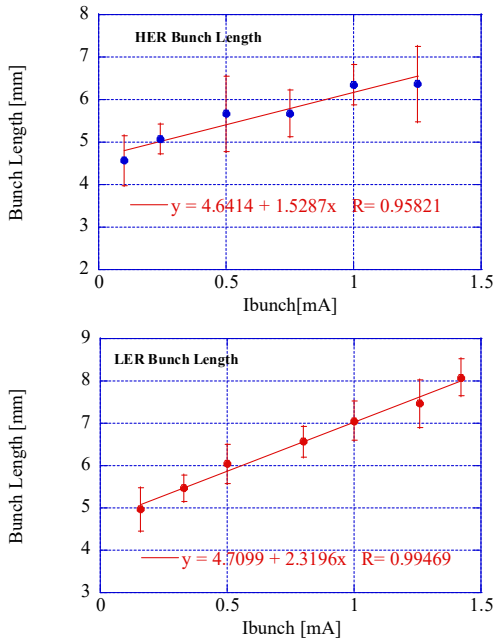

Figure 13: Measured bunch length of HER (upper) and LER (lower) with bunch current.

The bunch lengthening behaviour in HER is consistent with the KEKB because most of the vacuum chamber in arc and straight section have been re-used for SuperKEKB. Though the bunch lengthening in LER is moderated than that of measured in phase 1, it still shows unexpected larger lengthening with bunch current. We will need to find the impedance model to reproduce the behaviour.

The large angle beamstruhlung monitor (LABM) [16] installed just outside the QCS magnets have been commissioned during the phase 2 period. Though it seems still affected by large SR background, the analysis is in progress.

Beam Loss Monitor

For phase 2 operation, we have replaced the damaged PIN-diode monitors and cables especially around the beam collimators. For newly installed collimators we have added PIN diode monitors both to protect the collimators and to monitor and optimize the beam loss at the collimator. By the requirement from the commissioning team and the Belle II group, we have tuned the gain and the threshold value of beam abort. The fine beam loss value before the beam abort has been recorded using multi-channel fast data loggers. After the suspicious beam abort such as QCS quench we have checked the beam loss behaviours with the change of the cavity voltages and the change of DCCT value to find the real cause of the abort [17].

To abort the beam when the orbit has excursed wildly with high beam current operation to protect the vacuum chambers, we have prepared orbit abort system using Libera Brilliance+ in both rings with two BPM position per ring with the betatron phase advance around 90 deg. We have also recorded the post-mortem data of Libera (X, Y and intensity) when the beam position has changed to be out of the threshold value (± 2 mm). Though during phase 2 operation we did not enable this abort, the post-mortem

ISBN: 978-3-95450-201-1 doi:10.18429/JACoW-IBIC2018-MOOB01

data was useful also to confirm the beam orbit and the intensity just before the abort. As the current BPM for this abort has been selected in the dispersion free section, we plan to add the BPM with large dispersion to record the energy change just before the abort.

SUMMARY

Beam instrumentation systems for SuperKEKB rings, especially in the positron damping ring, have been constructed and commissioned. All the system has shown excellent performance and helped to realize smooth beam commissioning of the rings. With the experience of phase 2 operation, we will improve the instrumentation to be much useful to realize the performance of the SuperKEKB collider.

The authors would like to express their sincere appreciation to the commissioning group of SuperKEKB for their help in the operation.

This work is partly supported by the US-Japan collaboration in High Energy Physics (R&D for SuperKEKB and the next generation high luminosity colliders).

REFERENCES

[1] Y. Funakoshi *et. al.,* in *Proc. of IPAC'16*, Korea, Busan, 2016, paper TUOBA01.

[2] M. Tobiyama *et. al*, in *Proc. of IBIC'16*, Spain, Barcelona, 2016, paper MOAL03.

[3] Y. Onishi *et al.*, in *Proc. of IPAC'18*, 2018, Vancouver, BC, Canada.

[4] A. Morita *et al*., in *Proc of ICHEP'18,* Korea, Seoul, 2018, paper TUOBA01.

[5] H. Ikeda *et al.*, presented at IBIC'18, China, Shanghai, paper MOPA02, this conference.

[6] M. Tobiyama, in *Proc. of IBIC'14*, USA, CA, Monterey, USA, 2014.

[7] M. Tobiyama et al., in *Proc. of IBIC'17*, USA, MI, Grand Rapids, 2017, paper TUPCF09.

[8] M. Tejima, in *Proc. of IBIC'15* , Australia, Melbourne, 2015, paper TUBLA01.

[9] M. Tobiyama, *et al*., in *Proc. of PASJ'16*, Japan, Chiba, 2016, paper TUOM06.

[10] M. Tobiyama *et al.*, in *Proc. of IBIC'15*, Australia, Melbourne, 2015, paper MOPB018.

[11] H. Sugimoto *et al.,* in *Proc. of IBIC'17* , USA, MI, Grand Rapids, 2017, paper TU3AB1.

[12] M. Masuzawa, *et al.*, presented at IBIC'18, China, Shanghai, paper, this conference.

[13] DimTel, http://www.dimtel.com/

[14] E. Mulyani, *et al*., Submitted to NIM A.

[15] E. Mulyani, *et al*., in *Proc of IPAC'18*, Canada, BC, Vancouver, 2018, paper THPWL074.

[16] R. Ayad *et al*., arXiv:1709.01608.

[17] H. Ikeda *et al*., in *Proc. of IBIC'16*, Spain, Barcelona, 2016, paper TUAL03.